# Fabric Defect Detection and Classification Using Image Analysis

YIXIANG FRANK ZHANG[1] AND RANDALL R. BRESEE[2]

*The University of Tennessee, Knoxville, Tennessee 37996, U.S.A.*

ABSTRACT

Conventional image analysis hardware was used to image solid-shade, unpatterned, woven fabrics. Two different software approaches for detecting and classifying knot and slub defects were studied and compared. The approaches were based on either gray level statistics or morphological operations. The autocorrelation function was used for both methods to identify fabric structural repeat units, and statistical or morphological computations were based on these units. Plain weave and twill weave fabrics were used to compare the performance of each software approach.

Inspection for quality control purposes is important in textile manufacturing. Fabric defects are usually detected by human inspectors, a subjective, tedious, and time-consuming process. Recent advances in imaging technology have resulted in inexpensive, high quality image acquisition, and advances in computer technology allow image processing and pattern recognition to be performed quickly and inexpensively. Thus, automated image-based inspection offers an attractive alternative to human inspection.

Image-based inspection systems have been developed and used in a number of industries, including electronics, automobiles, lumber, and metal processing. Image-based techniques also have been investigated for textile manufacturing and testing. Studies include trash evaluation in cotton [15], fiber characterization [11, 20], blend irregularity in yarns [16], pile-fiber distribution in sliver-knitted fabrics [5], nonwoven structure characterization [3, 8, 10], carpet texture evaluation [14, 17-19], fabric testing [2, 6, 7, 9], and fabric defect detection [1, 12, 13]. Studies of fabric defect detection have been based primarily on gray level statistical approaches, and we have located no studies based on morphological approaches. In addition, the rationale for selecting the size and shape of the image area processed during defect detection has not been clear.

In this study, we considered two approaches to fabric defect detection and characterization—statistical and morphological methods. We developed an inspection procedure involving training and detection steps for each approach. During the training stage, we examined defect-free fabrics to determine nominal fabric structural repeat units and then based our statistical or morphological computations on these units. We examined fabrics containing defects to develop defect models. During the detection stage, we inspected fabrics using image areas of various size and shape to detect deviations from nominal fabric structure, classify these as knots or slubs, measure their size, and record their locations.

Both software approaches can detect and classify knots and slubs in solid-shade, unpatterned, woven fabrics illuminated by transmitted light. Knots are physically caused by entanglement of yarns. When fabrics are illuminated by transmitted light, these are identified visually as approximately symmetrical dark regions, which are substantially larger than individual yarns in fabrics. Slubs are physically caused by a coarse yarn, double pick, or double end. These are identified visually as elongated dark regions, which are substantially thicker than individual yarns in fabrics.

## Image Processing Methods

We used several techniques to process images for this study, including histogram equalization, autocorrelation, thresholding, erosion, dilation, and object classification.

### HISTOGRAM EQUALIZATION

Histogram equalization reassigns gray level values of pixels to achieve a more uniform gray level distribution in an image. During this process, individual

[1] Department of Computer Science. Current address: American Management Systems, Inc., Arlington, Virginia

[2] Center for Materials Processing.

pixels retain their brightness order, but a more flattened histogram is produced so the brightness and contrast of images are altered. Different images usually become more comparable to one another after histogram equalization, since their brightness and contrast are more similar. In many cases, histogram equalization provides an image with structural detail that is more discernible to the human eye than original image areas where small brightness gradients exist.

## AUTOCORRELATION

Autocorrelation is a technique that combines all parts of an image and may be used to characterize repetitive structures. In this project, we used autocorrelation to determine the weft and warp repeat lengths in fabric images. The autocorrelation functions in weft $C_{x,o}$ and warp $C_{o,y}$ directions are

$$C_{x,o} = \sum_i \sum_j X_{i,j} X_{i-x,j}$$

and

$$C_{o,y} = \sum_i \sum_j X_{i,j} X_{i,j-y} \quad , \qquad (1)$$

where $x_{i,j}$ is the gray level of pixel $(i,j)$ in an image. $C_{x,o}$ and $C_{o,y}$ exhibit maxima at integer multiples corresponding to the number of pixels comprising the average repeat unit size in each fabric direction. The intensity of these maxima would be expected to remain constant if the repeat unit in a fabric image were perfectly replicated throughout the image. On the other hand, the intensity of maxima would be expected to decrease with increasing rapidity as the perfection of repeat unit replication decreased. Consequently, autocorrelation provides a convenient means to determine both the average dimensions of repeat units and the perfection of repeat unit replication in fabric images.

## THRESHOLDING

The goal of image segmentation is usually to label image areas as either of two objects, such as fibers and pores or defects and defect-free areas. A common approach to segmenting an image is to use gray level thresholding, a process that compares the gray level of each image area with a given gray level (threshold), and labels each area as white if its gray level is greater than the threshold and black otherwise. The goal of threshold selection for this project was not only to label all defect areas as black to preserve the size and shape of defects, but also to label the minimum number of defect-free image areas as black.

Threshold selection is critically important, and many ways to perform this task have been devised [4]. Of course, choosing an appropriate image area to threshold is important. For our project, we subjected two different image areas to thresholding. For the first, we compared the gray level of individual pixels to the threshold gray level. For the second, we thresholded windows composed of many pixels by computing the mean gray level of pixels in the window and then comparing this mean to the threshold gray level. In order to select the size and shape of the window in a logical manner, we used the autocorrelation process to determine the fabric structural repeat unit and thresholded an image window equal in size and shape to this repeat unit.

We computed thresholds $T$ for either individual pixels or groups of pixels in windows using the following expression:

$$T = \mu + z\sigma \quad . \qquad (2)$$

The parameter $\mu$ represented either the mean gray level of individual pixels in defects or the global mean among window mean gray levels in defect-free fabrics. The parameter $\sigma$ represented the standard deviation of individual pixels in defects or the standard deviation of window mean gray levels in defect-free fabrics. We chose the factor $z$ somewhat by trial and error to determine the strictness of the defect detection test.

## EROSION AND DILATION

In this project, we used the common morphological operations of erosion, dilation, and opening (erosion followed by dilation). These operations involve simply adding or removing pixels from a binary image according to rules that depend on the pattern of neighboring pixels.

Let $Z^2$ denote the set of all ordered pairs of elements $(a,b)$, with $a$ and $b$ being integers from the set of real integers $Z$. Suppose that object $A$ and structuring element $B$ are represented as sets in $Z^2$. Let $(B)_x$ denote the translation of $B$, so its origin is located at $x$, and let $\hat{B}$ denote the reflection of $B$ so that

$$\hat{B} = (x \mid x = -b, b \subseteq B) \quad . \qquad (3)$$

The erosion of $A$ by structuring element $B$, denoted as $A \ominus B$, is defined as the set of all points $x$ such that $(B)_x$ is included in $A$. That is,

$$A \ominus B = (x \mid (B)_x \subseteq A) \quad . \qquad (4)$$

The dilation of $A$ by the structuring element $B$, denoted as $A \oplus B$, is defined as the set of all points $x$ such that $(B)_x$ and $A$ have a nonempty intersection. That is,

$$A \oplus B = (x|(\hat{B})_x \cap A \neq \phi) \quad , \qquad (5)$$

where $\phi$ denotes the empty set.

Of course, selecting the size and shape of the structuring element is a key step in morphological operations. Our goal for this project was to select an element large enough to erode windows associated with small deviations from the nominal fabric structure, but small enough to retain defects in the eroded image. We used the autocorrelation process to determine the size and shape of fabric structural repeat units. The unit size and shape in turn guided selection of the structuring element size and shape.

### Window Separation and Defect Classification

Once defective windows are detected, windows that belong to the same defect must be grouped to determine the size and shape of each defect. Since defects are more likely to occur along the warp and weft directions than along diagonal fabric directions, we used the city-block distance to determine the distance separating defective windows. Let $p$ and $q$, with coordinates $(x,y)$ and $(s,t)$, denote two defective windows in an image. The city-block distance between $p$ and $q$, $D_4$, is defined as

$$D_4(p,q) = |x - s| + |y - t| \quad . \qquad (6)$$

Once we determined window separation, we then classified windows. A defective window that had no neighbor located nearby (*e.g.*, $D_4 \geq 8$) was necessarily smaller than the size of individual yarns and was ignored. Windows that were grouped near at least one other window were classified as either knots or slubs, depending on their shape. If the length of a window group was more than twice its width, it was classified as a slub; otherwise, it was classified as a knot.

## Experimental Procedure

Images were acquired using a personal computer (386sx), frame grabber (PCvision plus), video camera equipped with a zoom lens, video monitor, and system monitor. Woven fabrics obtained from a local textile mill were illuminated with transmitted brightfield light provided by an overhead projector. An image was acquired by the video camera, digitized with $512 \times 480$ spatial and 8-bit gray level resolution, stored in frame grabber memory, and displayed on the video monitor. Acquired images were transferred to a Sun SPARC2 Unix workstation for processing.

We examined two methods of processing images for detecting knots and slubs—a gray level statistical approach and a morphological approach. Both involved a training stage and a testing stage. The general flow of processing for these approaches is shown in Figure 1.

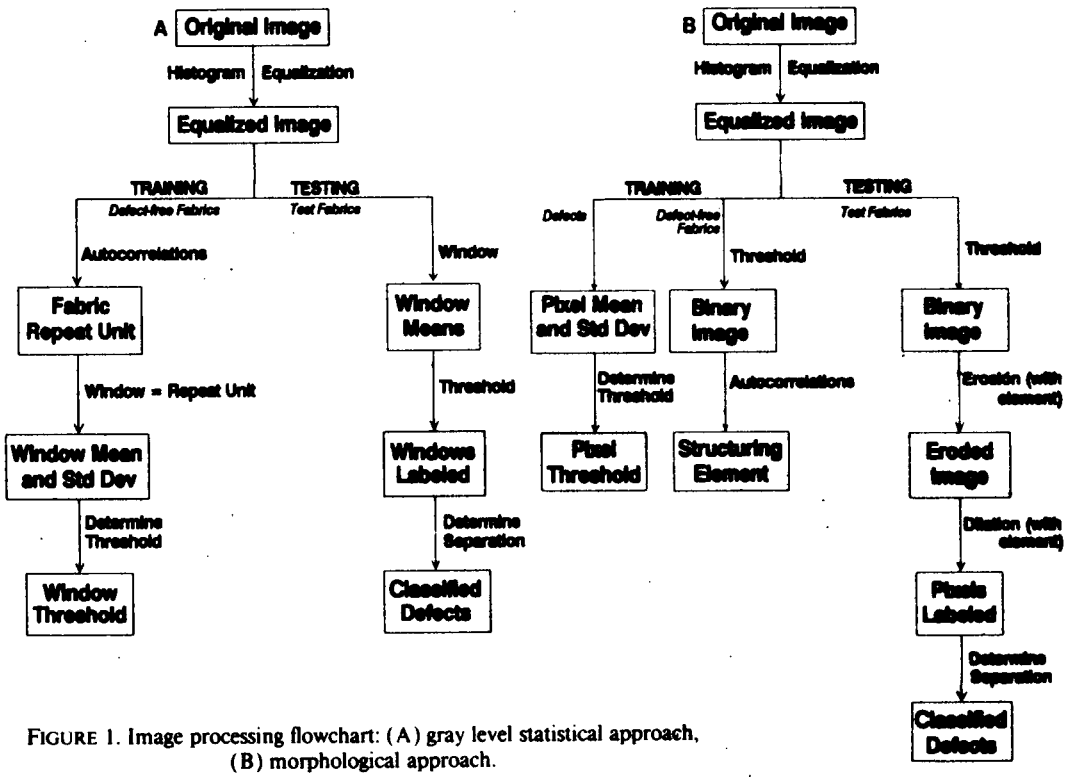


FIGURE 1. Image processing flowchart: (A) gray level statistical approach, (B) morphological approach.

### GRAY LEVEL STATISTICAL APPROACH

As illustrated in Figure 1A, all acquired images were first histogram equalized. Experiments showed that this was advantageous for two reasons. First, autocorrelation maxima and minima were more clearly identifiable in equalized images than in images not equalized. Second, images were more comparable after equalization, since their contrast and brightness were more similar. Consequently, a single threshold could be applied more successfully to equalized images than images not equalized.

The training stage involved the following steps: The nominal size of the fabric repeat unit in the warp and weft directions was determined from autocorrelations described by Equation 1 using a defect-free fabric sample. The size and shape of the window for subsequent processing were set equal to the size and shape of the nominal fabric repeat unit. The gray level mean among pixels within each window was computed and the global mean and standard deviation among windows as well. The threshold gray level was computed statistically using Equation 2 after a value of $z$ had been selected by trial and error to control the strictness of the test in a satisfactory manner.

The testing stage involved the following steps: A test fabric image was divided into windows of size and shape determined during the training stage. The gray level mean was computed for each window and compared to the threshold gray level determined during the training stage. If the window gray level mean was less than the threshold, the window was labeled defective; otherwise the window was labeled defect-free. Once defective windows were located, window separation was determined using Equation 6, and window groups were classified as either slub or knot defects.

### MORPHOLOGICAL OPERATION APPROACH

As illustrated in Figure 1B, all acquired images were first histogram equalized for the reasons discussed previously. The training stage involved the following steps: Fabric samples containing defects were imaged, and then the gray level mean and standard deviation among pixels in defective image areas were computed. The threshold gray level was computed statistically using Equation 2 after selecting a value of $z$ by trial and error to control the strictness of the test in a satisfactory manner. A defect-free fabric sample was imaged and thresholded to a binary image, and then the nominal size of the fabric repeat unit in the warp and weft directions was determined from autocorrelations described by Equation 1. The size and shape of this unit guided selection of the structuring element size and shape for subsequent morphological operations.

The testing stage involved the following steps: A test fabric image was thresholded pixel by pixel to produce a binary image. The binary image was subjected to erosion and then dilation using a structuring element determined during the training stage. This process located defective pixels in the fabric image. Once defective pixels were located, window separation was determined using Equation 6 and window groups were classified as either slub or knot defects.

## Results and Discussion

Figure 2 shows a histogram equalized image and the result of performing autocorrelations of this image in the weft ($C_{x,0}$) and warp ($C_{0,y}$) directions. As expected, the autocorrelations exhibit maxima when $x$ and $y$ equal 0. Additional peaks appearing at $x$ = 9, 18, 27, and at $y$ = 11, 22 indicate that the nominal fabric repeat unit is 11 × 9 pixels (warp × weft). The intensity of the autocorrelations decreases with increasing values of $x$ or $y$, indicating that the repeat unit is not perfectly replicated in the image and pixel gray levels are more correlated with nearby than with remote counterparts. The rate of decline in autocorrelation intensity is less in the weft direction than in the warp direction, which indicates that the repeat unit in this fabric is replicated more perfectly in the weft than warp direction.

Knowing the size and shape of fabric repeat units can be useful in guiding selection of the size and shape of processing windows for defect detection. As discussed earlier, processing window size and shape does not seem to have been well justified in previous fabric defect studies. One of our objectives was to examine the effects of the processing window on defect detection. First, consider the case of a defect-free fabric with a perfectly periodic repeating structure. If the size and shape of the processing window is set equal to that of the fabric repeat unit, each window would exhibit the same mean gray level. For a fabric that is also perfectly periodic but contains defects, mean gray levels of defect-containing windows would be expected to differ from those of defect-free windows.

Of course, real fabrics possess less than perfect periodicity. Consequently, mean gray levels of windows are distributed over a range of values even when no defects exist. When defects are present, thresholding would be expected to detect more defective windows when the distribution of defect-free window mean gray levels is narrow. One would expect the number of defective windows successfully detected to decrease as the width of the distribution of defect-free window

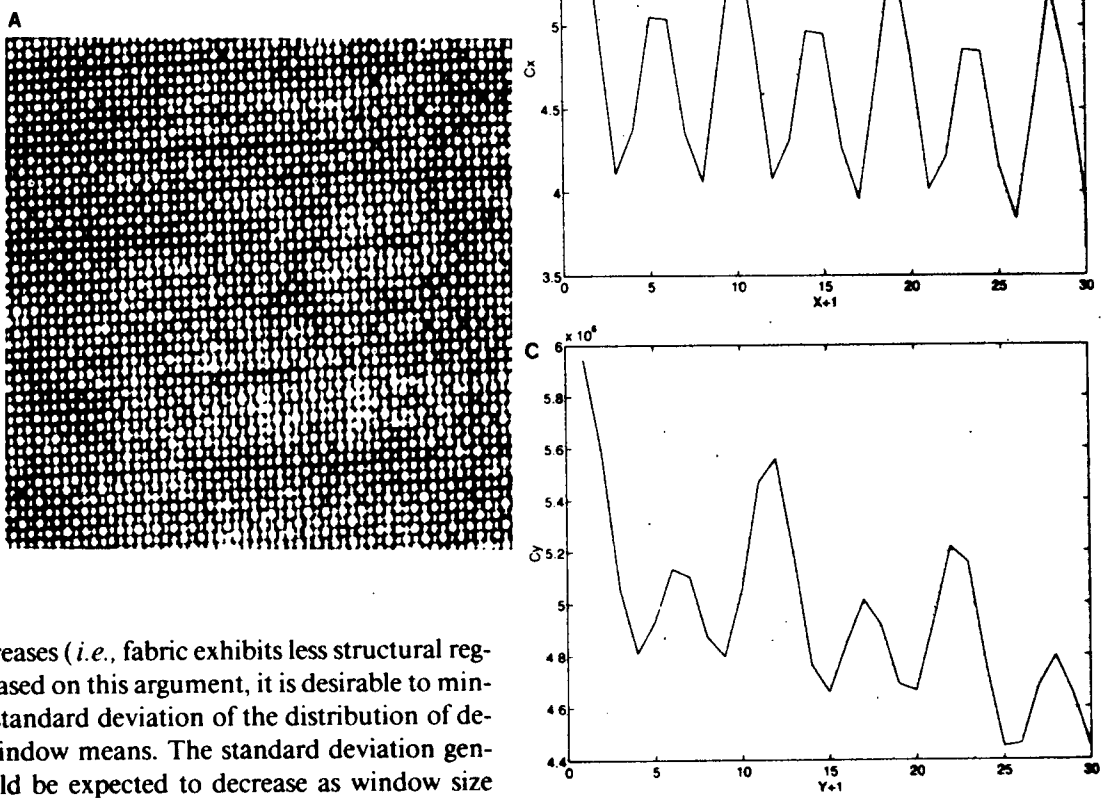


FIGURE 2. Autocorrelation: (A) fabric image, (B) weft-direction autocorrelation, (C) warp-direction autocorrelation.

means increases (*i.e.*, fabric exhibits less structural regularity). Based on this argument, it is desirable to minimize the standard deviation of the distribution of defect-free window means. The standard deviation generally would be expected to decrease as window size increases, since variations in fabric structure and thus pixel gray levels are physically averaged in larger windows.

Averaging fabric structural variations by using larger windows also decreases the ability to detect defects, however, since these are averaged along with defect-free structural units. Increasing window size must be balanced against the ability to detect important defects. It is logical to set the size and shape of the processing window equal to that of the fabric structural repeat unit. For the case of defect-free fabrics, the standard deviation of mean gray levels of such windows would be expected to be small, since each repeat unit would exhibit similar mean gray levels. For the case of defective fabrics, however, defect-containing windows would be expected to exhibit mean gray levels that are generally distinguishable from defect-free windows, since the size of slubs and knots is comparable to the size of the fabric repeat unit.

The effect of window size on gray level statistics is illustrated in Table I for a defect-free plain weave fabric with a repeat unit of 11 × 9 pixels. This table shows that the standard deviation of window mean gray levels generally decreases with increasing window size. Since larger windows also would be expected to decrease the ability to detect defects, however, the data in Table I suggest that the optimum window size and shape may be equal to the fabric repeat unit size and shape.

TABLE I. Variation of window mean gray levels for windows of different size.

| Window size | Standard deviation | Window size | Standard deviation | Window size | Standard deviation |
|---|---|---|---|---|---|
| 11 × 2 | 42.7 | 2 × 9 | 32.0 | 9 × 9 | 15.1 |
| 11 × 4 | 17.6 | 4 × 9 | 19.7 | 10 × 10 | 14.8 |
| 11 × 6 | 18.5 | 6 × 9 | 16.0 | 11 × 11 | 14.8 |
| 11 × 8 | 15.4 | 8 × 9 | 16.3 | | |
| 11 × 9 | 13.6 | 10 × 9 | 14.1 | | |
| 11 × 10 | 14.2 | 11 × 9 | 13.6 | | |
| 11 × 12 | 13.7 | 12 × 9 | 13.6 | | |
| 11 × 14 | 12.8 | 14 × 9 | 13.5 | | |

As we discussed earlier, selecting threshold values for image segmentation is critically important. Equation 2 can be used to compute threshold values from gray level distributions. This equation allows the strict-

ness of the test to be controlled conveniently by $z$. A small $z$ value limits the range of gray levels that are labeled normal. This increases the chance of correctly classifying defects as defects, but also increases the chance of incorrectly classifying normal structures as defects in the gray level statistical approach. Since real fabrics exhibit small deviations from the nominal fabric structure that are not associated with defects, this could result in serious errors. On the other hand, a large $z$ value labels a smaller range of gray levels as defective. Fewer normal structures are incorrectly labeled as defects, but more defects may be misclassified as normal. Consequently, a value of $z$ must be selected somewhat by trial and error during the training stage to optimize classification performance.

This process is illustrated for a plain weave fabric in Table II. Four specimens containing defects and five defect-free specimens were prepared from one roll of fabric. As the value of $z$ decreased, the number of knots and slubs detected in defective windows increased and the number of normal windows falsely classified as defects increased.

The effects of erosion and dilation on defect detection are illustrated in Figure 3. Figure 3A shows an image previously subjected to histogram equalization and thresholding. This image was then subjected to erosion using a 6 × 6 pixel structuring element, and the result is shown in Figure 3B. The structuring element was larger than dark elements associated with the nominal fabric repeat unit, so only the large thick slub in the center of the image remained in the eroded image. However, the size of the slub was reduced considerably by the erosion process. Figure 3C shows the result of dilating Figure 3B using a 6 × 6 pixel structuring element; the size of the slub in Figure 3B has been increased to a size similar to that in the original image (Figure 3A).

As discussed previously, selecting the size and shape of the structuring element is the key to morphological operations such as erosion and dilation. An element should be large enough to erode windows associated with small deviations from the nominal fabric structure, but small enough to retain important defects in the eroded image. Since autocorrelation can be em-

TABLE II. Classification performance for different threshold values for a plain weave fabric.

| | | $T = \mu - 3.60\sigma$ | | $T = \mu - 3.54\sigma$ | | $T = \mu - 3.10\sigma$ | |
|---|---|---|---|---|---|---|---|
| Specimen number | Defect type | Defective windows detected | Normal windows misclassified | Defective windows detected | Normal windows misclassified | Defective windows detected | Normal windows misclassified |
| 1 | slub | 14 | 0 | 15 | 0 | 17 | 0 |
| 2 | slub | 4 | 0 | 6 | 0 | 12 | 3 |
| 3 | slub | 7 | 0 | 8 | 0 | 11 | 2 |
| 4 | knot | 5 | 1 | 5 | 2 | 5 | 3 |
| 5 | none | 0 | 0 | 0 | 0 | 0 | 1 |
| 6 | none | 0 | 0 | 0 | 0 | 0 | 1 |
| 7 | none | 0 | 0 | 0 | 0 | 0 | 1 |
| 8 | none | 0 | 0 | 0 | 0 | 0 | 2 |
| 9 | none | 0 | 0 | 0 | 0 | 0 | 1 |
| Total | | 30 | 1 | 34 | 2 | 45 | 11 |

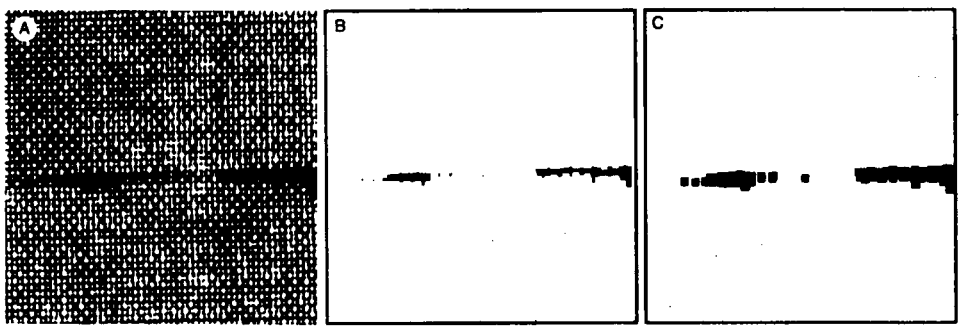


FIGURE 3. Erosion and dilation: (A) original image, (B) image after erosion, (C) image after erosion and then dilation.

ployed to determine the size and shape of the nominal fabric repeat unit, it can be used for selecting the structuring element size and shape. Figure 4 shows the results of autocorrelation for a defect-free twill fabric image after equalization and thresholding. The location of autocorrelation maxima indicates that the nominal repeat unit for this fabric is 15 × 6. On the other hand, the minima suggest that the separation between bright and dark sections of the image is 8 × 3. This suggests, in turn, that the minimum effective structuring element size might be 8 × 3. Figure 5 shows an equalized and thresholded image of the twill fabric corresponding to the data of Figure 4; it contains a single slub defect. The image was subjected to opening by elements of different size. We can see that opening with structural elements smaller than 8 × 3 results in nondefective fabric structures not being fully eroded from the original image. These results indicate that autocorrelation may be used to determine the minimum effective structuring element for performing morphological operations with fabrics.

The overall ability of the gray level statistical approach to detect and correctly classify defects is summarized in Table III, which shows test results for nine plain and twill weave fabrics. All of the slubs (15 out of 15) and most of the knots (13 out of 15) were detected and correctly classified. In addition, the number of defect-free samples incorrectly labeled as containing a defect was small (1 out of 43).

The overall ability of the morphological approach to detect and correctly classify defects in the same nine plain and twill weave fabrics is summarized in Table IV. All of the slubs (15 out of 15) and most of the knots (14 out of 15) were detected and correctly classified. However, the number of defect-free samples incorrectly labeled as containing a defect was substantial (6 out of 43).

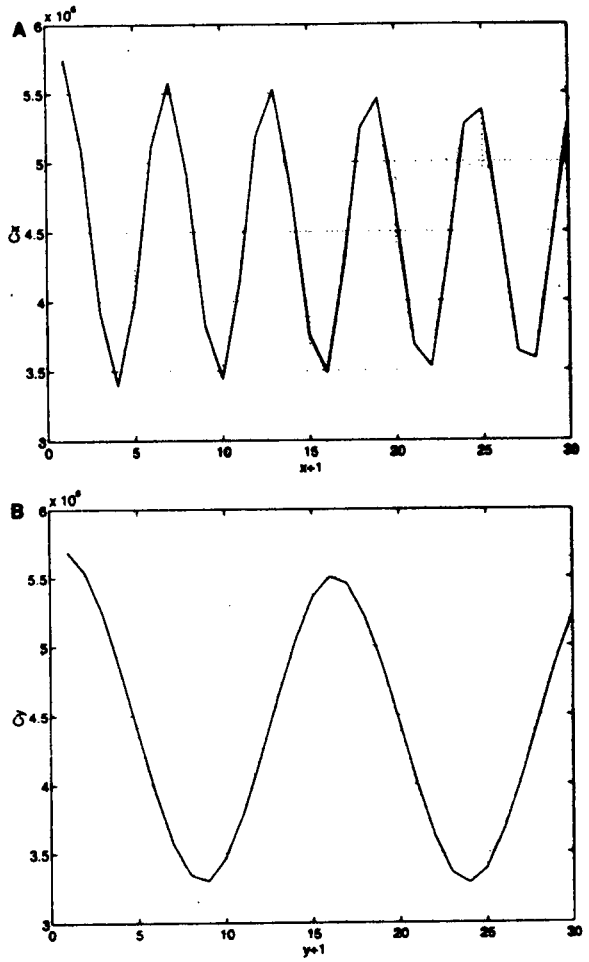


FIGURE 4. Autocorrelation of a defect-free twill fabric: (A) weft-direction autocorrelation, (B) warp-direction autocorrelation.

The gray level statistical approach offered advantages compared to the morphological approach. First, the gray level approach was faster because it involved fewer

TABLE III. Results of gray level statistical testing.

| Fabric samples | | Defects present | | Defects detected | | Defect-free specimens | Defects detected |
|---|---|---|---|---|---|---|---|
| | | Slubs | Knots | Slubs | Knots | | |
| Plain weaves | A | 3 | 1 | 3 | 1 | 5 | 0 |
| | B | 1 | 1 | 1 | 1 | 6 | 0 |
| | C | 2 | 0 | 2 | 0 | 6 | 0 |
| | D | 1 | 3 | 1 | 3 | 4 | 0 |
| | E | 2 | 2 | 2 | 1 | 4 | 0 |
| Twill weaves | F | 2 | 2 | 2 | 2 | 4 | 0 |
| | G | 3 | 1 | 3 | 1 | 4 | 0 |
| | H | 0 | 4 | 0 | 3 | 4 | 1 |
| | I | 1 | 1 | 1 | 1 | 6 | 0 |
| Total | | 15 | 15 | 15 | 13 | 43 | 1 |

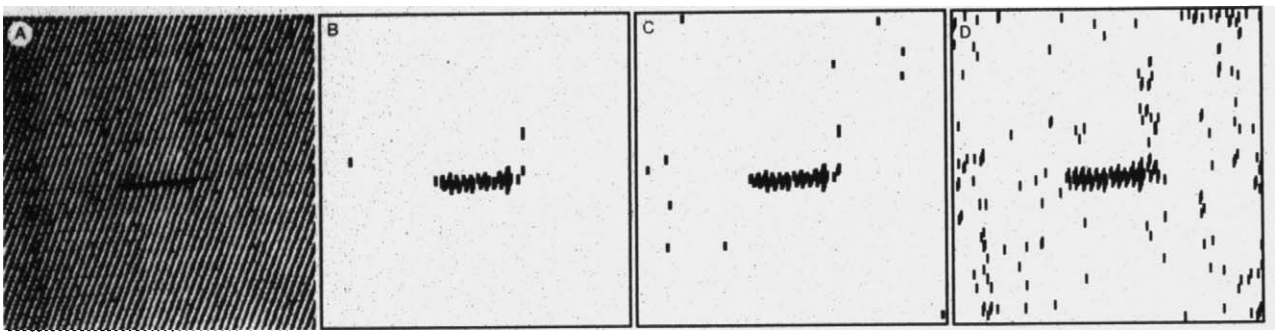


FIGURE 5. Opening a defect-containing twill fabric using structural elements of varying size: (A) original image, (B) after opening with size = 8 × 3, (C) after opening with size = 7 × 3, (D) after opening with size = 8 × 2.

TABLE IV. Results of morphological testing.

| Fabric samples | | Defects present | | Defects detected | | Defect-free specimens | Defects detected |
|---|---|---|---|---|---|---|---|
| | | Slubs | Knots | Slubs | Knots | | |
| Plain weaves | A | 3 | 1 | 3 | 1 | 5 | 0 |
| | B | 1 | 1 | 1 | 1 | 6 | 0 |
| | C | 2 | 0 | 2 | 0 | 6 | 0 |
| | D | 1 | 3 | 1 | 3 | 4 | 3 |
| | E | 2 | 2 | 2 | 1 | 4 | 2 |
| Twill weaves | F | 2 | 2 | 2 | 2 | 4 | 0 |
| | G | 3 | 1 | 3 | 1 | 4 | 0 |
| | H | 0 | 4 | 0 | 4 | 4 | 1 |
| | I | 1 | 1 | 1 | 1 | 6 | 0 |
| Total | | 15 | 15 | 15 | 14 | 43 | 6 |

processing steps and combined pixels into larger windows so thresholding required fewer computations. Second, fewer defect-free specimens were falsely determined to be defective using the gray level approach, apparently because windows containing several pixels were thresholded in the gray level approach, whereas individual pixels were thresholded in the morphological approach. This may have made the gray level approach more noise tolerant, because noise in individual pixels would be expected to contribute more to false image segmentation when individual pixels are thresholded than when windows containing several pixels are thresholded.

Although the morphological approach was slower and produced more false positives than the statistical approach, it was inherently sensitive to defect size and shape. For our project, we chose a structuring element for erosion and dilation that was designed to eliminate small deviations from the nominal fabric structure and detect all other deviations. Alternatively, one could select a structuring element that only detects those defects exceeding some specific size or shape. For example, if one were only interested in large slubs, the width and length of the structuring element could be increased to retain only these defects and erode all others. Discriminating among various defects in this manner could reduce the number of false positives produced by the morphological approach. Nevertheless, a higher quality image is required for the this approach than for the statistical approach, because image noise would still be expected to contribute more to false image segmentation since individual pixels rather than windows containing several pixels are thresholded.

## Conclusions

We studied and compared two image analysis-based approaches for detecting knots and slubs in solid-shade, unpatterned woven fabrics. For defect detection with gray level statistics, we used autocorrelation to determine the nominal fabric repeat unit size and shape. Processing window size and shape was set equal to that of the fabric repeat unit. Image segmentation used window threshold values based on gray level statistics from defect-free fabrics. For defect detection by morphological operations, we examined defects to determine pixel threshold values and used autocorrelation to determine the structural element size and shape for

morphological operations. Test fabric images were thresholded and defects detected by erosion followed by dilation.

We compared the performance of both methods by testing nine plain and twill weave fabrics. Both methods exhibited similar abilities to detect and correctly classify slub and knot defects, but fewer defect-free specimens were falsely determined as defective using the gray level approach. This apparently resulted because the gray level approach was more noise tolerant, since it involved thresholding windows rather than individual pixels as in the morphological approach.

ACKNOWLEDGMENTS

We thank Michael Thomason and Jens Gregor for technical advice and Cherokee Textile Mill for providing the fabrics used in this study.

## Literature Cited

1. Andrews, L., Contribution Concerning the Detection of Defects on Small-Patterned Textiles, *Melliand Texilber.* **72,** 981–984 (1991).
2. Cheng, L., and Bresee, R. R., Appearance Evaluation by Digital Image Analysis, *Textile Chem. Color.* **22,** 17–19 (1990).
3. Gong, R. H., and Newton, A., Image-analysis Techniques Part I: The Measurement of Pore-size Distribution, *J. Textile Inst.* **83,** 253–268 (1992).
4. Gonzalez, R. C., and Woods, R. E., "Digital Image Processing," Addison-Wesley Publishing Co., Reading, MA, 1992.
5. Harlock, S. C., and Gisbourne, D. N., An Image-analysis Technique Applied to the Measurement of the Pile-fibre Distribution in Sliver-knitted Fabric, *J. Textile Inst.* **80,** 585–593 (1989).
6. Hinze, D., and Mehlhorn, H., Objective Assessment of the Warp Stripiness of Woven Fabrics by Means of Digital Image Processing, *Melliand Texilber.* **73,** 33–36 (1992).
7. Hinze, D., Mehlhorn, H., and Burkhardt, S., Digital Image Processing by Means of a Parallel Computer System for the Testing of Fabrics, *Melliand Texilber.* **72,** 993 (1991).
8. Huang, X.-C., and Bresee, R. R., Characterization of Nonwoven Web Structure Using Image Analysis Techniques, Part I: Pore Analysis in Thin Webs, Part II: Fiber Orientation Analysis in Thin Webs, Part III: Web Uniformity Analysis, *J. Nonwovens Res.* **5**(1), 13–21, **5**(2), 14–21, **5**(3), 28–38 (1993).
9. Kaasjager, A. D. J., Textile Fabric Monitoring with Image Analysis, *Melliand Texilber.* **71,** 64–66 (1990).
10. Pourdeyhimi, B., and Xu, B., Pore Size Characterization in Nonwoven Fabrics, *J. Nonwovens Res.* **5**(3), 20–27 (1993).
11. Robson, D., Weedall, P. J., and Harwood, R. J., Cuticular Scale Measurements Using Image Analysis Techniques, *Textile Res. J.* **59,** 713–717 (1989).
12. Rösler, U., Defect Detection of Fabrics by Image Processing, *Melliand Texilber.* **73,** 635–636 (1992).
13. Schicktanz, K., Practical Experience with Automatic Cloth Inspection by the Laser-scan System, *Melliand Texilber.* **71,** 786–789 (1990).
14. Sobus, J., Pourdeyhimi, B., Gerde, J., and Ulcay, Y., Assessing Changes in Texture Periodicity Due to Appearance Loss in Carpet: Gray Level Co-occurence Analysis, *Textile Res. J.* **61,** 557–567 (1991).
15. Taylor, R. A., Estimating the Size of Cotton Trash with Video Images, *Textile Res. J.* **60,** 185–193 (1990).
16. Watanabe, A., Kurosaki, S.-N., and Konda, F., Analysis of Blend Irregularity in Yarns Using Image Processing, Part I: Fundamental Investigation of Model Yarns, *Textile Res. J.* **62,** 690–696 (1992).
17. Wood, E. J., Applying Fourier and Associated Transforms to Pattern Characterization in Textiles, *Textile Res. J.* **60,** 212–220 (1990).
18. Wu, Y., Pourdeyhimi, B., and Spivak, S. M., Texture Evaluation of Carpets Using Image Analysis, *Textile Res. J.* **61,** 407–419 (1991).
19. Wu, Y., Pourdeyhimi, B., Spivak, S. M., and Hollies, N. R. S., Instrumental Techniques to Quantify Textural and Appearance Changes in Carpet, Part IV: Colorimetric Image Analysis, *Textile Res. J.* **60,** 673–687 (1990).
20. Xu, B., Pourdeyhimi, B., and Sobus, J., Characterizing Fiber Crimp Using Image Analysis: Definitions, Algorithms, and Techniques, *Textile Res. J.* **62,** 73–80 (1992).

*Manuscript received January 13, 1994, accepted June 9, 1994*